Performance study of phase change materials coupled with three-dimensional oscillating heat pipes with different structures for electronic cooling

Ling, Yun-Zhi; Zhang, Xiao-Song; Wang, Feng; She, Xiao-hui

DOI:
10.1016/j.renene.2020.03.008

Journal Pre-proof

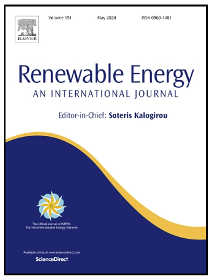

Performance study of phase change materials coupled with three-dimensional oscillating heat pipes with different structures for electronic cooling

Yun-Zhi Ling, Xiao-Song Zhang, Feng Wang, Xiao-hui She

PII: S0960-1481(20)30322-0
DOI: https://doi.org/10.1016/j.renene.2020.03.008
Reference: RENE 13148

To appear in: *Renewable Energy*

Received Date: 22 June 2019
Accepted Date: 02 March 2020

Performance study of phase change materials coupled with three-dimensional oscillating heat pipes with different structures for electronic cooling

Yun-Zhi Ling*[1], Xiao-Song Zhang[1], Feng Wang[2], Xiao-hui She[3]

[1]School of Energy and Environment, Southeast University, Nanjing210096, China
[2]College of Electrical, Energy and Power Engineering, Yangzhou University, Yangzhou 225127, PR China
[3]School of Chemical Engineering, University of Birmingham, Birmingham B15 2TT, UK
** Corresponding author. Tel/Fax: +86 - 15150567036.*

E-mail address: yunzhiseu@outlook.com

Abstract: E*lectronic cooling* has been a rising issue mainly due to the rapid development of high-throughput computing in data centres as well as battery energy storage, which release huge amount of heat through compact surfaces. The electronic cooling process is not only energy-intensive but also difficult to control. This paper proposes an effective cooling method for electronic devices by integrating phase change materials (PCMs) with three-dimensional oscillating heat pipes (3D-OHPs), where PCMs are used to store heat dissipated by the electronic device and 3D-OHPs to fast transport the stored heat from PCMs to the environment. A novel leaf-shaped structure is designed for the 3D-OHPs. Experimental study is carried out on the leaf-shaped 3D-OHPs with various working parameters including cooling air velocity, wind direction and heat input. Further, the leaf-shaped 3D-OHPs are embedded into PCMs to cool down the electronic devices. Temperature variations and thermal resistance are evaluated and compared with the conventional air cooling method. The experimental results indicate that the surface temperature of electronic devices can be well controlled below 100 ^{o}C, which is ~35 ^{o}C lower than that with conventional air cooling. The thermal resistance is decreased up to 36.3%. The 3D-OHPs with a filling ratio of 34-44% achieve the best thermal performance. What's more, the leaf-shaped structure of the 3D-OHPs contributes to a ~2 ^{o}C lower temperature on the electronic device's surface than the typical used 3D-OHPs. This research will promote the development of effective cooling for electronic devices.

Keywords: Thermal energy storage, heat pipe, phase change material, electronic cooling, thermal management

Nomenclature

Bo	Bond number
d	Diameter [m]
g	Gravitational acceleration [m/s^2]
h	Convective heat transfer coefficient $[\mathrm{W/(m^2 \cdot K)}]$
i	Number of measuring points
k	Thermal conductivity $[\mathrm{W/m \cdot K}]$
L	Length [m]
Nu	Nusselt number
Pr	Prandtl number
Q	Heat power [W]
r	Radius [m]
R	Thermal resistance $[\mathrm{°C/W}]$
s	Pitch of the pipe [m]
Re	Reynolds number
t	Time [s]
$\overline{T}$	Mean temperature [°C]

Acronyms

FR	Filling ratio
LSOHP	Leaf-shaped oscillating heat pipe
PCM	Phase change material

Greek symbols

ε	*Correction factor*
λ	Heat conductivity $[\mathrm{W/(m^2 \cdot K)}]$
ρ	Density [kg/m^3]
σ	Surface tension [N/m]
φ	Cooling efficiency

Subscripts

b	base
c	condensation
cc	wall of the copper case
e	evaporation
f	ambient
h	electronic component simulator
l	liquid
m	medium
o	contact
s	steady state
v	vapor

1. Introduction

The increasing demand for powerful electronic devices have a high requirement on effective cooling solutions capable of dissipating heat sufficiently. This is especially challenging to existing facilities with the current trend of miniaturization. Thus, effective electronic cooling is in urgent demand. Thermal energy storage with phase change materials (PCMs) can absorb and release thermal energy for peak-load shifting as well as reducing the system capacity[1]. This type of energy storage unit has been adopted in electronic cooling and ventilation applications[2][3]. With phase change materials, a significant temperature reduction in the operating temperature of electronic devices can be achieved, which significantly improves their performance and enhances stability[4]. However, the low thermal conductivity limits the application of phase change materials[5][6].

The recent reports focused on using heat pipes to enhance the heat transfer performance [7]. Table 1 shows the reported cooling method using PCMs coupled with heat pipes in electronic cooling. In addition, heat pipe-based cooling system was also used in thermal management of battery energy storage [12], which was considered as a promising solution [13].

Table 1 PCM coupled with heat pipe applied in electronic cooling in recent literature

Researchers	PCM	Material-working fluid	Power	Method
Behi et al. (2017)[8]	RT-42	Copper-water	Variable	Numerical study
Weng et al. (2011)[1]	Tricosane	Copper-water	Variable	Experimental study
Krishna et al. (2017)[9]	Tricosane/ Al_2O	Copper-water	Variable	Experimental study
Zhao et al. (2016)[10]	Paraffin	Copper-water	Variable	Experimental study
Qu et al. (2015)[11]	Paraffin	Copper-water	Variable	Experimental study

An oscillating heat pipe (OHP) is an effective thermal transmission device, which has a great potential for the application in electronic cooling. The oscillating heat pipe, also called pulsating heat pipe, was first introduced by Akachi [14] in the 1990s. A typical OHP is an interconnected capillary tube with many turns that is partially filled with a working fluid [15]. During the operation, continuous condensation (in the condenser) and evaporation (in the evaporator) of the working fluid produce a pressure difference that drives the fluid motion in the channel; liquid plugs and vapor slugs are alternately distributed along the pipe[16]. Compared with the traditional heat pipe, the OHP is a passive heat transfer device that exhibits several unique operating features such as high heat transport capability and manufacturing flexibility. The oscillating heat pipe has been used and studied widely[17][18].

The two-dimensional oscillating heat pipe (2D-OHP) is a device that is commonly applied in many fields because of its simple structure, flexible operation, and good applicability. However, the heat transmission direction of the 2D-OHP is limited to a flat plane. The mounting direction also limits the utilization of the 2D-OHP. The three-dimensional oscillating heat pipe (3D-OHP) was designed for highly integrated electronic components to enhance the thermal management. It involves more heat transmission directions than the 2D-OHP. It also improves the temperature distribution of the electronics, making it more uniform.

The thermal performance of 3D-OHP has been investigated in several previous studies. Qu et al. [19] demonstrated that the start-up temperature and thermal resistance of the 3D-OHP depended on the cooling air velocities and operating orientation. Ma et al. [20] proposed several flat-plate 3D-OHPs and tested the temperature oscillations and thermal resistance under different conditions. A multi-layered Ti–6Al–4V OHP (ML-OHP) was designed by Ibrahim [21] and was experimental studied to characterize its thermal performance under different conditions. The results indicated that the ML-OHP can be effectively operated while being filled with several working fluids and was almost independent of the operation orientation and gravity. Thompson et al. [22] investigated the performance of flat-plate 3D-OHPs. They reported that the amplitude of temperature oscillations depended on the heating width, operating orientation, and working fluid properties.

The flow structure of natural systems may provide ideas for the design of new types of 3D-OHPs. Bejan et al. [23] published a book about the design in nature as a scientific discipline. They focused on discovering a physics law for the design in nature. The branching networks had been investigated by several researchers to study the hydrodynamics and thermodynamics. Rubio-Jimenez et al. [24] designed flow channel structures for heat sinks. They demonstrated that Ψ-shaped configurations resulted in a reduced thermal resistance and more uniform surface temperatures, compared with Y-shaped structures. Zhang et al. [25] studied the thermal and flow behaviors of bifurcations and bends in fractal-like microchannel networks. The results indicated that the pressure drop and heat transfer performance depended on the aspect ratio. Xu et al. [26] numerically investigated the flow and thermal performance of several tree-shaped microchannel networks with and without loops. They reported that tree-shaped nets with loops improved the performance of the electronic cooling system. Convective heat transfer is important for devices with a branching structure. Luo et al. [27] provided a theoretical expression to calculate the convective heat transfer rate and reported that symmetrical branches resulted in a large heat transfer rate when the trunk diameter was larger than 0.004 m. Nayak et al. [28] also performed a three-dimensional numerical simulation to investigate the pressure drop and heat transfer coefficient in a Y-shaped branch pipe with a 60° branch angle. Zheng et al. [29] studied the solidification behavior in the heat exchanger with different fin configurations and found that the tree-shaped fins has significant influence on the enhancement of the PCM solidification.

The above literature review shows that the thermal performance of three-dimensional oscillating heat pipes (3D-OHPs) was studied under different conditions. However, the optimal structure design was seldom reported. The structural design of branching networks for electronics cooling has drawn much attention, while it has never been applied on the 3D-OHPs. With the inspiration of leaf shapes, this paper proposes a leaf-shaped three-dimensional oscillating heat pipes (LSOHPs) for improving heat transfer performance. Further, the LSOHP is embedded into phase change materials to cool down electronic devices. Experimental study is conducted with various working parameters and significant temperature decreases on the surface temperature of electronic devices are observed, indicating efficient electronic cooling.

2. Experiment

2.1 Experimental setup of oscillating heat pipes

In this study, typical three-dimensional oscillating heat pipes (3D-OHPs) were designed, fabricated, and tested in the laboratory. The OHPs were fabricated using red copper. The height of a 3D-OHP was 180mm. The length and width of a 3D-OHP with 8 turns were both 90 mm. Fig.1 shows a schematic of the geometry of the 3D-OHPs and the points measured during the test. Deionized water was used as the working fluid; the filling ratio (FR) was changed from 24% to 54%.

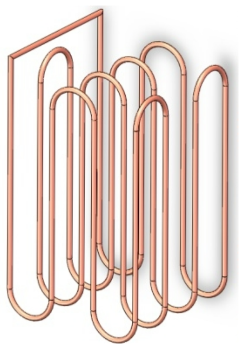

a) schematic

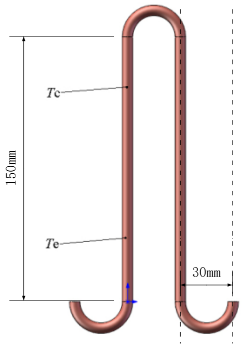

b) geometry of the turn

c) picture of a typical 3D-OHP

Figure 1 Schematic of the three-dimensional oscillating heat pipe (3D-OHP) and the points measured during the test

The thermally excited oscillating motion of the working fluid mainly depends on the surface tension and channel diameter. The internal diameter of the OHP must be small enough such that the liquid plugs can be separated by the vapor slugs. The formation of the liquid–vapor interface is characterized by the Bond number:

$$\mathrm{Bo} = \frac{r^2 g\left(\rho_l - \rho_v\right)}{\sigma} \tag{1}$$

where Bo is the bond number, r is the hydraulic radius of the pipe, ρ_l is the density of the liquid, ρ_v is the density of the vapor, σ is the surface tension, and g is the gravitational acceleration. Taft et al. [30] reported that a value of 0.85 can be used to calculate the maximum hydraulic radius of an OHP. The rearrangement of Eq. (1) shows that the maximum radius of the microchannel embedded in an OHP system is:

$$r_{h,\max} \leq 0.92\sqrt{\frac{\sigma}{g\left(\rho_l - \rho_v\right)}} \tag{2}$$

The limit of the pipe diameter can be defined using Eq. (2). In this study, copper tubes charged with deionized water were fabricated. At 20℃， the maximum diameter of the 3D-OHP was 5.46 mm. The inner diameter of 3 mm and outer diameter of 5 mm were bent in a U-shape in this study.

The thermal performance including the temperature variations and thermal resistances of the 3D-OHPs under different working conditions were analyzed in detail.

The OHP was tested under heating powers in the range of 25 to 100 W. The thermal resistance can be defined by Eqs.(3)-(5). The parameters $\overline{T_e}$ and $\overline{T_c}$ are the mean temperatures of the evaporation and condensation sections [°C], respectively:

$$\overline{T}_e = \frac{1}{8}\sum_{i=1}^{8} T_{ei} \tag{3}$$

$$\overline{T}_c = \frac{1}{8}\sum_{i=1}^{8} T_{ci} \tag{4}$$

$$R = \frac{\left(\overline{T}_e - \overline{T}_c\right)}{Q} \tag{5}$$

where i is the index number of the measurement point. The temperature was measured using K-type thermocouples with a reading accuracy of ±0.75%.

A leaf-shaped 3D-OHP (LSOHP) was designed. Fig.2 shows a schematic of the LSOHP. The height of the LSOHP was 180 mm. The length (L) and width (W) of the LSOHP with 8 turns were 150 and 85 mm, respectively. Deionized water was used as the working fluid; the filling ratio was 44%.

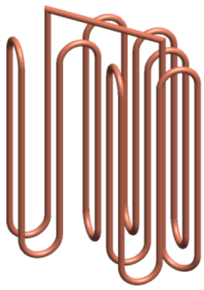

a) schematic geometry

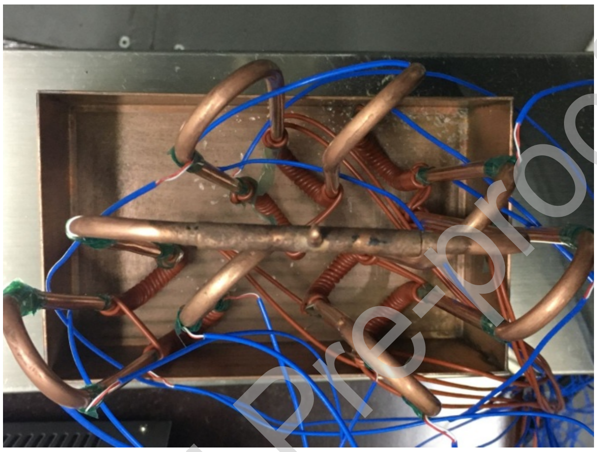

b) picture of the LSOHP (top-view)

Figure 2 Schematic of the leaf-shaped three-dimensional oscillating heat pipe (LSOHP)

The constructal law was defined to design the LSOHP. As shown in Fig.3 a), the transform angle (a_t) was 45°. The evaporation section of a LSOHP has eight turns, which were defined as the evaporation branches. To describe the design, a sketch of the virtual branches is shown in Fig. 3 b). Combined with the virtual branches, the top view of the LSOHP is shaped like a piece of a leaf. According to the constructal law of a LSOHP, three structural parameters were used: the transform angle a_t, number of the evaporation branches Ψ_e, and number of the condensation branches Ψ_c. The values of the parameters are shown in Table 2.

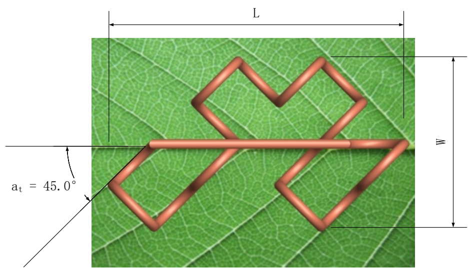

a) geometry of the leaf-shaped 3D-OHP (top-view)

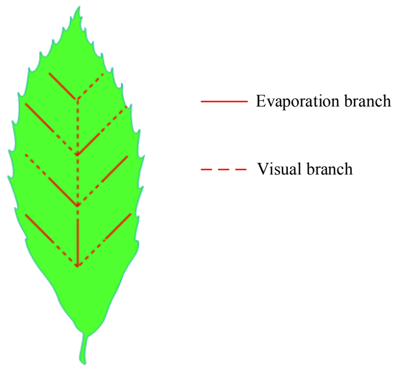

b) design thought of a LSOHP (top view)

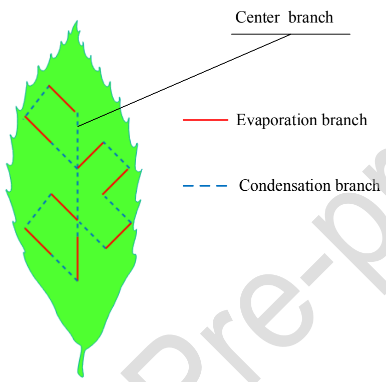

c) constructal law of a LSOHP (top view)

Figure 3 Design and constructal law of the leaf-shaped three-dimensional oscillating heat pipe (LSOHP)

Table 2 Structural parameters of the leaf-shaped three-dimensional oscillating heat pipe (LSOHP)

a_t	Ψ_e	Ψ_c
45°	8	7

To allow comparisons between different types of 3D-OHPs, similar geometric parameters, turn numbers, and filling volumes were used.

The 3D-OHP unit was tested in a controlled laboratory environment with a multipurpose air-cooling system. The ventilation mode and laboratory environment were controlled by the control cabinet. To control the ventilation mode, the control switch was adjusted; the obtained air distribution is shown in Fig. 4.

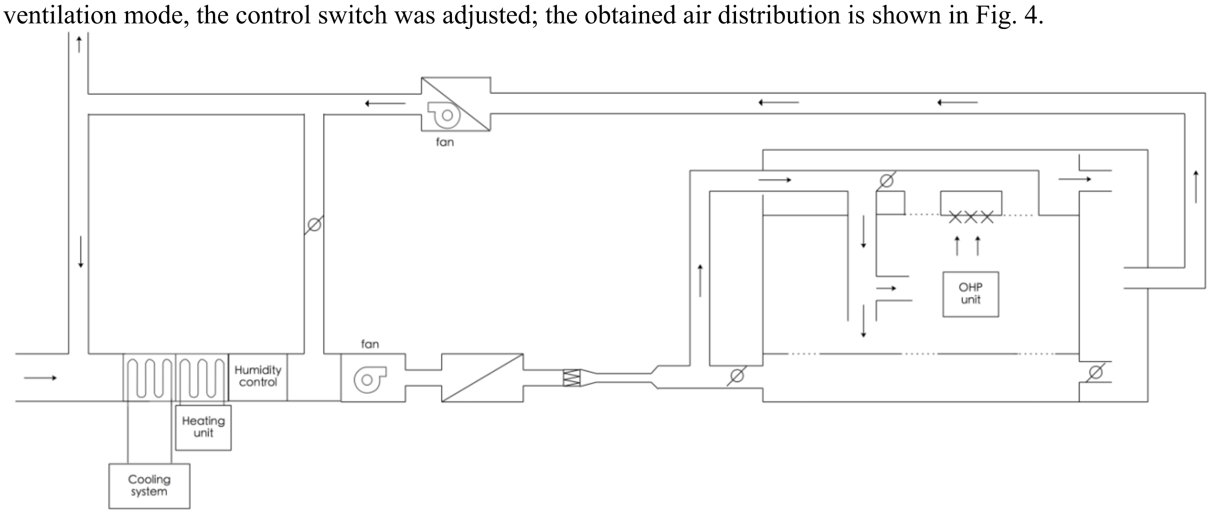

Figure 4 Schematic of the test room

The cooling air was supplied to the heat-retaining room by the duct in the ceiling plenum. After cooling of the OHP system, the air was returned from the ceiling plenum to the cooling system. The width and height of the air supply pipe were 600 and 150mm, respectively. The cooling air was controlled by the control cabinet and external fan with a specified temperature of 20°C.

Fig.5 illustrates the experimental apparatus of the OHP unit. Charensawan and Terdtoon reported that the thermal resistance depends on the evaporator length section. Decreasing the evaporator length improves the thermal performance for all cases of used tube diameters, FRs, and working fluids [31]. In this study, the lengths of the evaporation and condensation sections of the proposed 3D-OHPs were 50 and 60 mm, respectively. The temperature oscillation was studied in detail by deploying a single OHP unit into a thermal isolation box along with the heating elements. The box was filled with a glass wool insulation layer. The evaporation section of the 3D-OHP was wrapped with resistance heating wires. The heating power was controlled in the range of 25 to 100 W by adjusting the voltage transformer. The condensation section of the 3D-OHP was cooled by the air-cooling system.

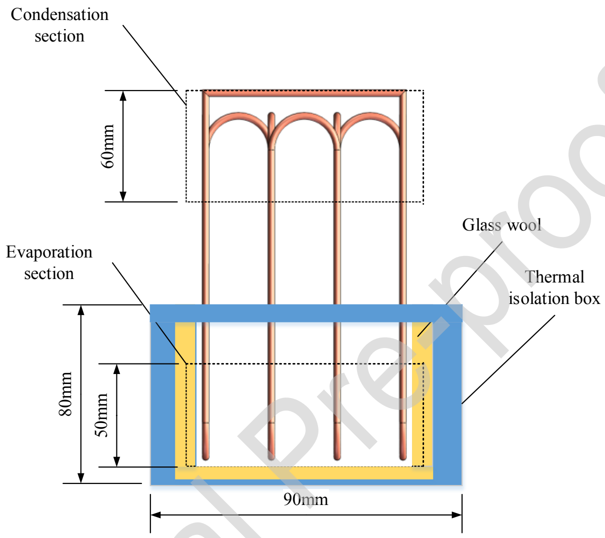

Figure 5 Experimental apparatus of the test unit for three-dimensional oscillating heat pipes (3D-OHP)

The effect of the wind directions on the thermal performance was studied by rotating the 3D-OHP to a fixed position. Then the cooling air flows through the 3D-OHP from different directions, as shown in Figs 6 and 7.

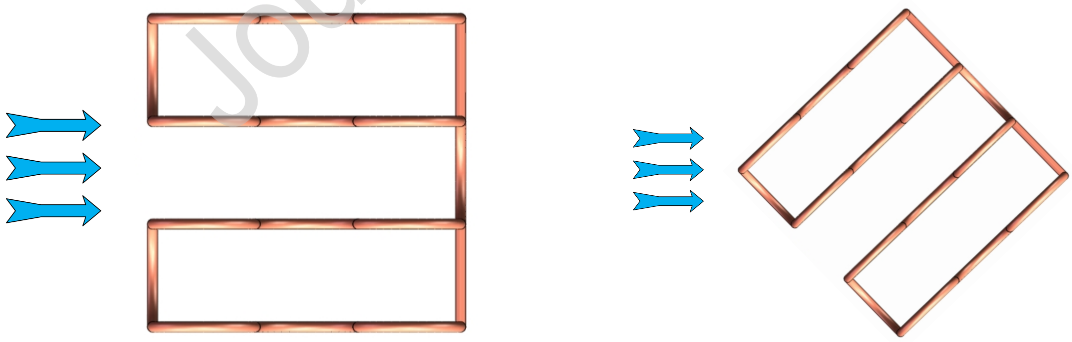

a) wind direction (forward flow) b) wind direction (side flow)

Figure 6 Wind direction of the three-dimensional oscillating heat pipes (3D-OHP)

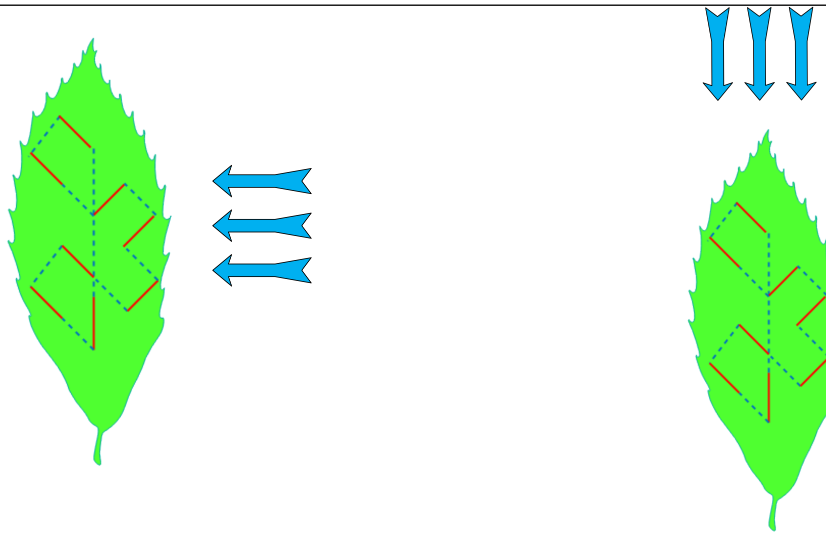

a) wind direction (side flow) b) wind direction (forward flow)

Figure 7 Wind direction of the leaf-shaped three-dimensional oscillating heat pipe (LSOHP)

2.2 Experimental setup of the PCM/OHP unit

In this study, the unit of phase change materials embedded with three-dimensional oscillating heat pipes (PCM/OHP) was designed to cool the electronic component simulator. The PCM/OHP unit consists of an aluminum heating platform, a copper case, and the paraffin wax along with the 3D-OHP. Fig.8 illustrates the experimental apparatus of the PCM/3D-OHP unit. The length and width of the copper case were 92 and 92mm, respectively.

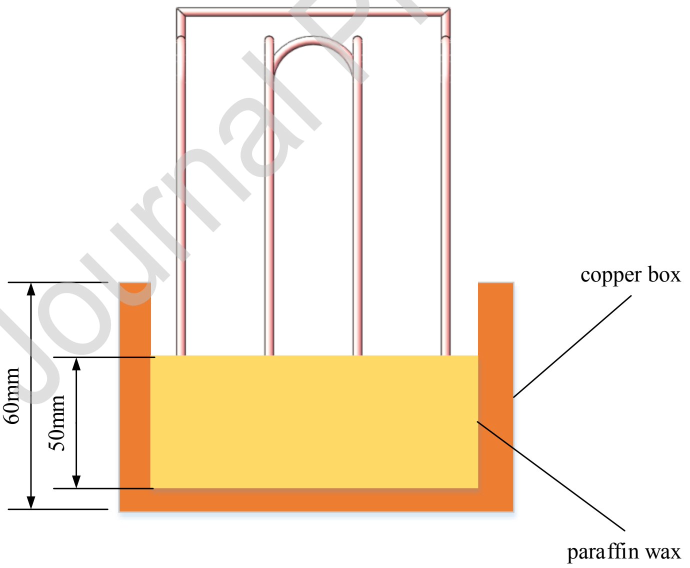

Figure 8 Schematic of the PCM/3D-OHP unit

The evaporation section of the 3D-OHP was inserted into the paraffin wax filled in the copper case and heated by the aluminum heating platform placed under the bottom of the case. The condensation section of the OHP is cooled by the air-cooling system in the insulated room. The main thermo-physical parameters of the paraffin wax were shown in Table 3. The aluminum heating platform was selected as the electronic component simulator. The heating power can be adjusted in the controller and the base temperature can be displayed in the monitor.

Table 3 Thermo-physical parameters of the paraffin wax

Parameters	Phase-transition temperature (℃)	Latent heat (J/g)	Thermal conductivity

			($W/m\cdot K$ for 20 ℃)
Values	52 ± 1	176.7	0.19

Under floor air distribution (UFAD) shown in Fig. 9 was adjusted to cool the PCM/3D-OHP unit in a controlled laboratory environment. The cooling air was supplied by the plenum to the heat-retaining room and drawn into the cabinet simulator by the AC frequency fan. After cooling of the PCM/OHP unit placed in the room, the air was returned from the ceiling plenum to the cooling system. The cooling air temperature was 22°C.

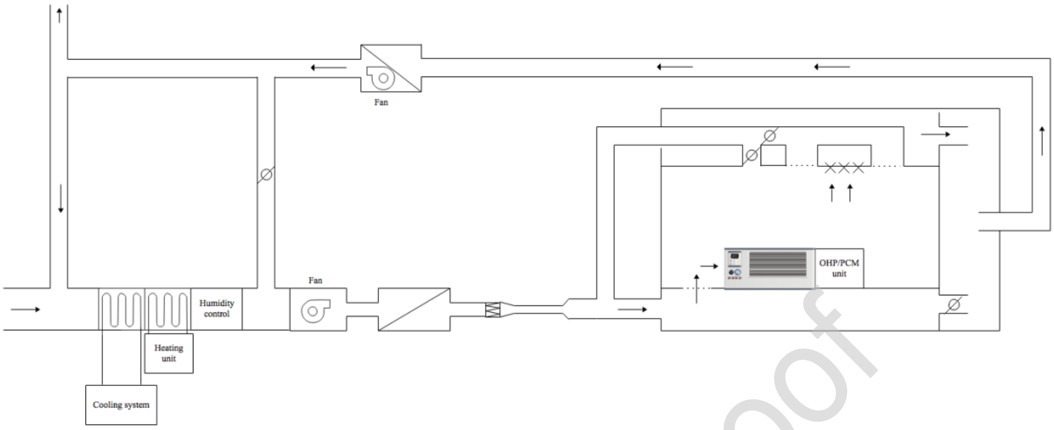

Figure 9 Schematic of the test room with under floor air distribution

Cooling performance of PCM/3D-OHP unit was studied under a heating power of 80W. The temperature distribution during melting process was calculated by the thermal imager (FLIR SC660) with an accuracy of $\pm 1\%$ of the reading. The pictures of the experimental devices including the thermal imager were shown in Fig. 10.

Figure 10 Schematic of the test room with under floor air distribution

The cooling efficiency, φ, is defined as:

$$\varphi = \frac{R_h - R_s}{R_h} \tag{6}$$

$$R_h = \frac{T_h - T_f}{Q} \tag{7}$$

$$R_s = \frac{T_s - T_f}{Q} \tag{8}$$

where R_h is the thermal resistance of the electronic component simulator without PCM/3D-OHP unit, R_s is the thermal resistance of the electronic component simulator coupled with the PCM/3D-OHP unit, T_h is the equilibrium base temperature of the electronic component simulator without PCM/3D-OHP unit, T_s is the equilibrium temperature of the electronic component simulator coupled with the PCM/3D-OHP unit, T_f is the ambient temperature, Q is the heat power.

3. Results and discussion

The temperature variations of the proposed three-dimensional oscillating heat pipes (3D-OHPs) were studied experimentally at heating powers ranging from 25 to 100 W. The temperatures of the evaporation and condensation sections were monitored and recorded.

3.1 Thermal performance of the three-dimensional oscillating heat pipe

3.1.1 Effect of the filling ratio on the 3D-OHP

Fig. 11 shows the oscillating temperature curves of the proposed 3D-OHPs. The oscillating temperature curves clearly indicate two periods. When the heating power is relatively low, no oscillation is observed. As the heating power increases, the heat flux by evaporation occurring at the liquid-vapor interface increases and the vapor volume variation acts as a spring in the system. The slug/plug flow formed and a thin layer of liquid film placed on the surface. As a result, the temperature oscillation presents a large fluctuation associated with an occasionally large amplitude and low frequency. The heating power at which a notable temperature oscillation can be observed was defined as the start-up power. The results show that the start-up power depends on the FR. When the FR is 34%, the start-up power is the lowest. This indicates that less power is required to initiate oscillations. When the FRs are decreased to 24% or increased to 54%, the start-up power significantly increases. This indicates that different FRs correspond to different thermally excited oscillating motions. At a FR ranging from 34% to 44%, a small heating power is required to initiate oscillations. At FRs beyond this range, more heat is required to generate an oscillating motion in the 3D-OHP.

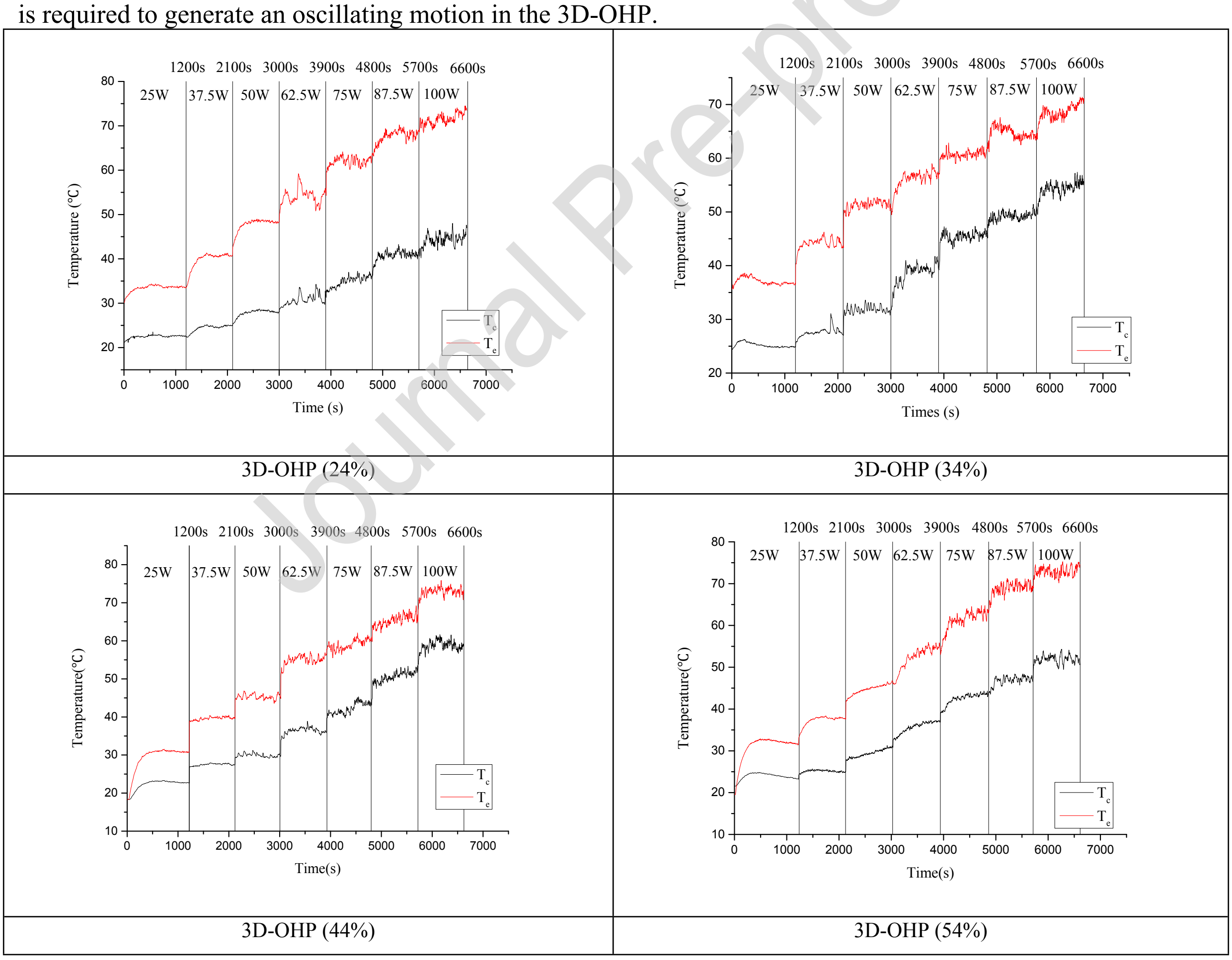

Figure 11 Temperature oscillations of the 3D-OHPs at different FRs

We assume that the heating power is constant (without any loss), the low temperature of the evaporation section indicates that the heat is rejected effectively. Therefore, the temperature of the evaporation section should be small enough to ensure that the electronic components work in the recommended range. The temperature variations of the 3D-OHPs under different FRs in the evaporation section are depicted in Fig. 12. At a high heating power in the range of 75 to 100W, the 3D-OHP with a FR of 34% exhibits the lowest temperature and the 3D-OHP with a FR of 44% exhibits the second lowest temperature. Because hot spots mostly occur when the electronic components are operated at a high heating power, a FR in the range of 34% to 44% is recommended to achieve a better cooling performance.

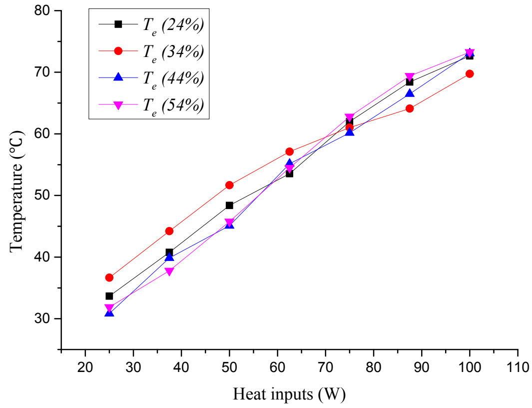

Figure 12 Temperature variations of the 3D-OHPs at different FRs in the evaporation section

Fig. 13 illustrates the thermal resistance of the 3D-OHPs at different heating powers depending on different FRs. In general, the thermal resistance decreases with increasing heating power. At a low heating power, the thermal resistance slowly decreases or even increases before it decreases. The inflection point is probably due to thin film evaporation phenomena. As the heating input increases, the slug/plug flow forms and a thin layer of liquid film develops on the surface. The thermal-excited oscillating motion is generated in the capillary tube, which significantly improves the forced convection in addition to the phase change heat transfer. Based on the results of 3D-OHPs charged with deionized water at different FRs, the thermal resistance presents a divergent trend when the heat input is relatively small (e.g., ≤ 50W). When the heat input is higher than 50W, the 3D-OHP with a FR in the range of 34% to 44% exhibits the lowest thermal resistance.

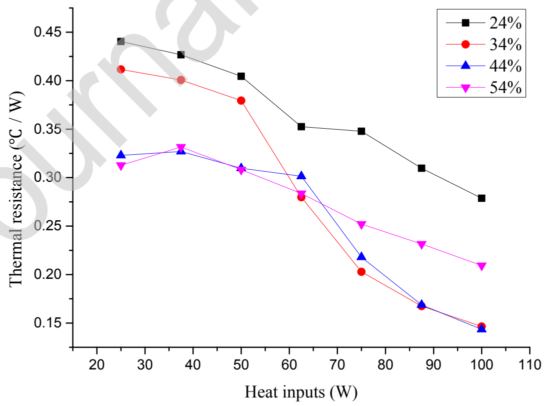

Figure 13 Thermal resistance of the 3D-OHPs at different FRs

The above-mentioned analysis shows that 3D-OHPs with filling ratios in the recommended range of 34% to 44% achieve the best thermal performance.

3.1.2 Effect of the cooling air velocities on the 3D-OHP

Fig. 14 shows the temperature curves of the 3D-OHP with a FR of 44% at different cooling air velocities. When the cooling air velocity increases from 5 to 8m/s, the temperatures of the evaporation and condensation sections notably decrease, which is probably due to the enhancement of the convective heat transfer.

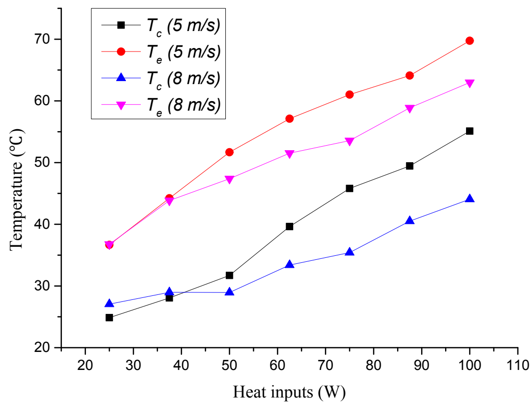

Figure 14 Temperature variations of the 3D-OHPs at different cooling air velocities

When the 3D-OHP is vertically placed, the cooling air is supplied from different directions. We consider the 3D-OHP as a tube bundle and neglect the effect of turns. As shown in Fig. 6 a), for the 3D-OHP in aligned arrangement, the Zhukauskas equation was used to calculate the Nusselt number ($Re = 10^3–2 \times 10^5$), i.e.,

$$Nu = \varepsilon_n 0.27 Re^{0.63} Pr_f^{0.36} (Pr_f/Pr_w)^{0.25} \tag{9}$$

where ε_n is the correction factor for the tube bundle. The correction factor was set to 0.910 in this case. The convective heat transfer coefficient can be determined as follows:

$$h = Nu \cdot \frac{\lambda}{d} \tag{10}$$

where λ is the heat conductivity and d is the outer diameter of the pipe. The convective heat transfer coefficients of the 3D-OHPs are 121.4 and $163.3 W/(m^2 \cdot K)$ when the velocities of the cooling air are 5 and 8m/s, respectively. The convective heat transfer coefficient increases with the increase of cooling air velocity. The temperatures of the condensation section decrease due to the enhancement of convective heat transfer.

As shown in Fig. 13, the thermal resistance at different cooling velocities show the same trend. And the difference between thermal resistance at different cooling velocities was small. The result demonstrated that the temperature of the evaporation section decreased with the increase of cooling air velocity. With respect to electronics cooling, we consider that the temperature of the evaporation section is one of the most important factors influencing the cooling performance. A high cooling air velocity benefits the cooling performance. However, increasing the cooling air velocity is accompanied by the increase in the energy consumption. An optimal trade-off between the cooling air velocity and temperature of the evaporation section should be made to ensure that the electronic components operate in the recommended temperature range with less energy consumption.

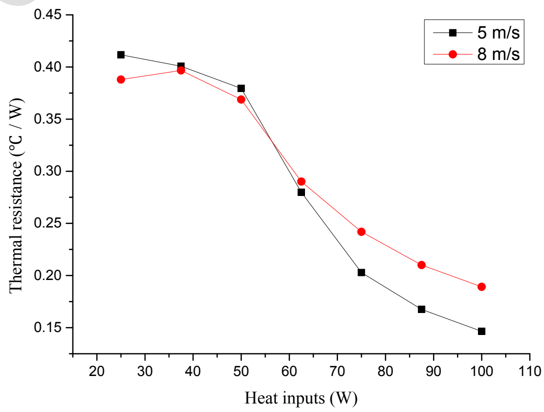

Figure 15 Thermal resistance of the 3D-OHPs at different cooling air velocities

3.1.3 Effect of the wind directions on the 3D-OHP

Fig. 6 shows the schematic of the 3D-OHP at different wind directions. Fig. 6a shows the flow of cooling air through the 3D-OHP in aligned arrangement; in this case, Eqs(9) and (10) can be adopted to calculate the convective heat transfer coefficient, that is, h=121 $W/(m^2 \cdot K)$. Fig. 6b illustrates the side flow through the 3D-OHP in staggered arrangement.

For the 3D-OHP in staggered arrangement shown in Fig. 16, the cooling air flowing through the curved passage alternately contracts and expands between the tubes. Therefore, the disturbance during the flow process is stronger than the cooling air flowing through the tube bundle in aligned arrangement, which leads to an enhanced heat exchange. Thus, the convective heat transfer coefficient of the 3D-OHP in staggered arrangement should be larger than the convective heat transfer coefficient of the 3D-OHP in aligned arrangement.

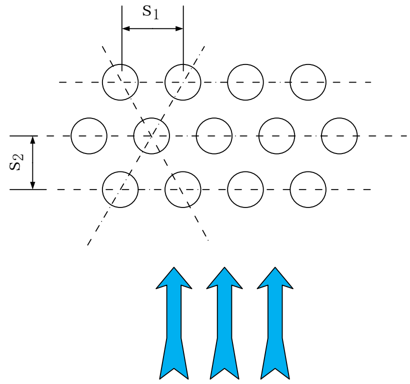

Figure 16 Air flow through the 3D-OHP in staggered arrangement

Fig. 17 shows that the 3D-OHP with side flow exhibits a lower evaporation temperature. This indicates that the temperature of the evaporation section decreases with increasing convective heat transfer coefficient. The thermal resistance has little change with different wind directions (Fig. 18).

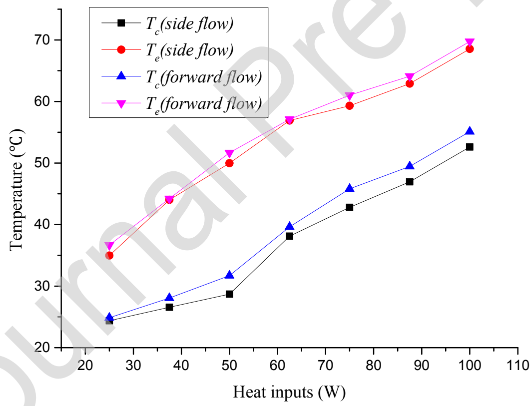

Figure 17 Temperature variations of the 3D-OHPs at different wind directions

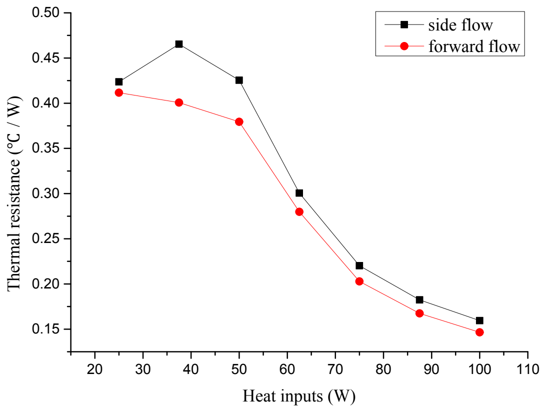

Figure 18 Thermal resistance of the 3D-OHPs at different wind directions

The combined study of the temperature variation and thermal resistance indicates that the cooling performance of the 3D-OHP depends on the wind direction. The 3D-OHP in staggered arrangement exhibits a better cooling performance.

3.2 Thermal performance of the leaf-shaped three-dimensional oscillating heat pipe

The above-mentioned analysis has proven that a filling ratio in the range of 34% to 44% leads to the best thermal performance. The 3D-OHP in staggered arrangement exhibits a better cooling performance. We assume that the flow structures found in natural systems may provide ideas for the design of new types of 3D-OHPs with better cooling performances. Therefore, we designed a leaf-shaped three-dimensional oscillating heat pipe (LSOHP), which has a complex structure. A LSOHP with a filling ratio of 44% was designed to study the influence of the structure on the cooling performance (Fig. 2).

3.2.1 Effect of the wind directions on the LSOHP

Fig. 19 shows the oscillating temperature curves of the proposed LSOHP. The oscillating temperature curves show that the start-up power was 50W. The start-up power was constant at different wind directions.

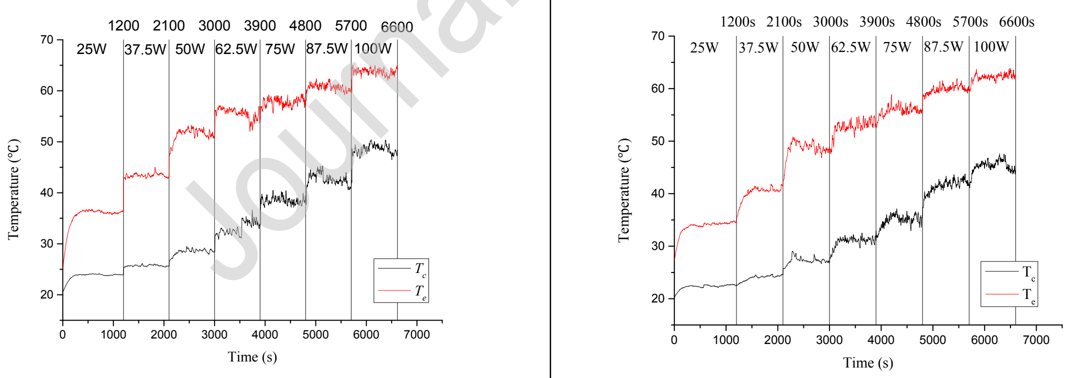

a) wind direction (side flow) b) wind direction (forward flow)

Figure 19 Temperature oscillations of the LSOHP at different wind directions

Figs20 and 21 illustrate the temperature variations and thermal resistance of the LSOHP for different wind directions. The LSOHP with forward flow exhibits a low temperature in the evaporation section. It indicates that the LSOHP with forward flow has a better cooling performance than the LSOHP with side flow.

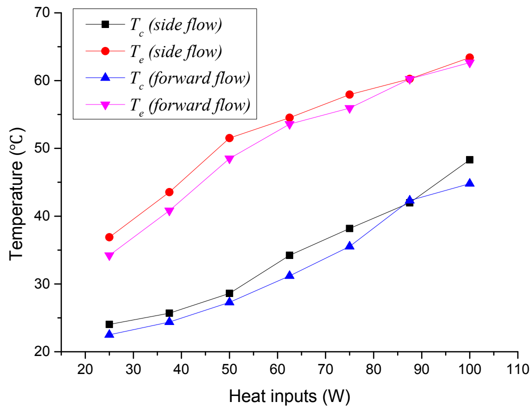

Figure 20 Temperature variations of the LSOHP at different wind directions

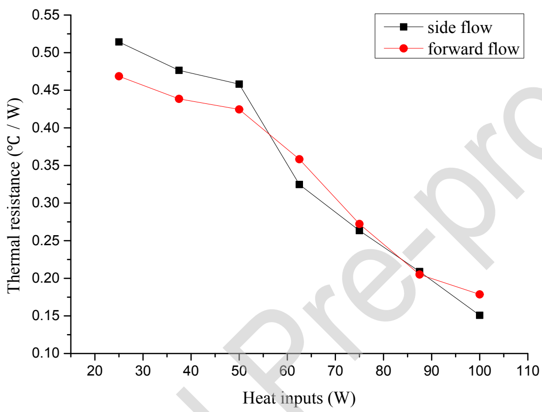

Figure 21 Thermal resistance of the LSOHP at different wind directions

For the LSOHP in staggered arrangement, the Zhukauskas equation was used to calculate the Nusselt number ($\mathrm{Re} = 10^3$–2×10^5):

$$Nu = \varepsilon_n \cdot 0.35\left(\frac{s_1}{s_2}\right)^{0.2} Re^{0.6} Pr_f^{0.36} (Pr_f/Pr_w)^{0.25} \tag{11}$$

where ε_n is the correction factor for the tube bundle. The correction factor was set to 0.928 and 0.965 for side and forward flow, respectively.

Eqs(10) and (11) were adopted to calculate the convective heat transfer coefficients. The convective heat transfer coefficients of the LSOHP were 132 and 137.3$\mathrm{W/(m^2 \cdot K)}$ when the wind directions were side and forward flow, respectively. Therefore, the temperature in the evaporation and condensation sections decrease with increasing convective heat transfer coefficient. The thermal resistance at different wind directions are approximately equal at a high heat input.

When the cooling air velocity was constant, the comparison between the temperature variations of the LSOHP and 3D-OHP shows that the LSOHP exhibits a lower temperature in the evaporation section. This indicates that the LSOHP has a better cooling performance than the typically used 3D-OHP.

3.2.2 Effect of the cooling air velocities on the LSOHP

Fig. 22 and Fig. 23 show the temperature variations and thermal resistance of the LSOHP. Eqs(10) and (11) were adopted to calculate the convective heat transfer coefficients. The convective heat transfer coefficients of the 3D-OHP are 132 and 170.3 $\mathrm{W/(m^2 \cdot K)}$ when the cooling air velocities are 5 and 8m/s, respectively. The results illustrate that the higher the convective heat transfer coefficient is, the lower is the temperature in the evaporation and condensation sections.

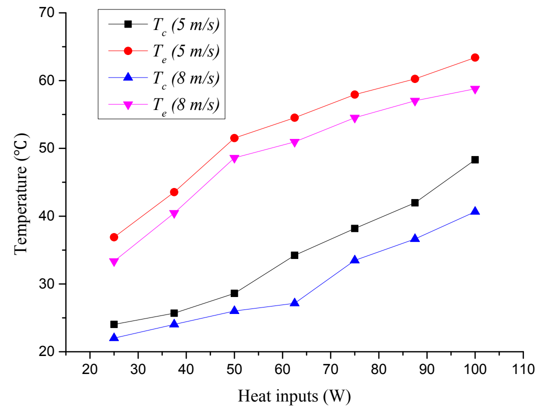

Figure 22 Temperature variations of the LSOHP at different air velocities

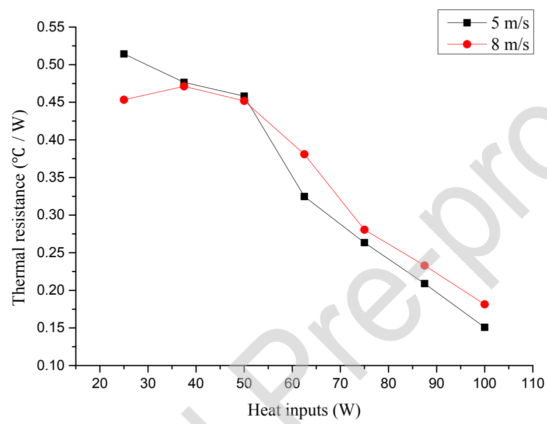

Figure 23 Thermal resistance of the LSOHP at different air velocities

As shown in Figs. 20 and 22, the temperature difference between the evaporation sections of the LSOHP at different wind directions is much smaller than the temperature difference between the evaporation sections of the LSOHP at different cooling air velocities. This is probably due to the varying convective heat transfer coefficient differences. When the convective heat transfer coefficient difference increases, the temperature difference between the evaporation sections increases.

3.3 Cooling performance of the phase change materials embedded with three-dimensional oscillating heat pipe

The phase change materials embedded with three-dimensional oscillating heat pipe (PCM/3D-OHP) is tested to study the cooling performance for electronic devices. The thermal resistance model is developed for the PCM/3D-OHP unit. The thermal resistance model is shown in Fig. 24. T_h is the temperature of the electronic component simulator, R_o is the thermal contact resistance, T_b is the base temperature of the copper case, R_m is the medium thermal resistance, T_{PCM} is the average temperature of the PCM shown in the thermal images, R_{cc} is the thermal resistance between the base of the copper case and the wall of the copper case, T_{cc} is the wall temperature of the copper case, $R_{\mathrm{cc-f}}$ is the thermal resistance between the wall of the copper case and the ambient temperature, T_{f} is the ambient temperature, R_c is the condensation thermal resistance, T_c is the temperature of the condensation section, $R_{\mathrm{c-f}}$ is the thermal resistance between the condensation section and the ambient temperature.

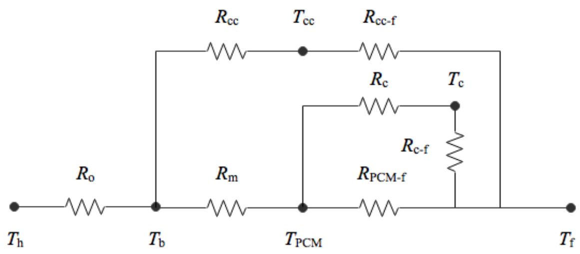

Figure 24 Thermal resistance model of the PCM/3D-OHP unit

We neglect the effect of the copper case on the cooling performance, then the thermal conductivity enhancement of the PCM using 3D-OHP can be determined by the temperature difference between the electronic component simulator and the average temperature of the PCM shown in the thermal images ($\Delta T_{\mathrm{PCM}} = T_h - T_{PCM}$). The total thermal resistance can be determined by Eqs. 7 and 8.

An investigation on the cooling performance of PCM coupled with 3D-OHP was conducted. The equilibrium temperature of the electronic component simulator was recorded. The temperature distribution of the PCM/3D-OHP unit was sketched by the thermal imager. The maximum and average temperatures are shown in the pictures.

When the electronic component simulator without PCM/3D-OHP unit was cooled by the air with a velocity of 5 m/s. The resulting base temperature, T_h, was 135 ℃ when the heating power was 80W.

Fig. 25 shows the internal temperature distribution of the copper case at different cooling air velocities. The equilibrium temperature of the electronic component simulator were 101 and 94 ℃ (a difference of 7 ℃) when the cooling air velocities were 5m/s and 8m/s, respectively. The calculated cooling efficiency was shown in Table 4. The results indicated that the cooling efficiency was significantly affected by the cooling air velocities.

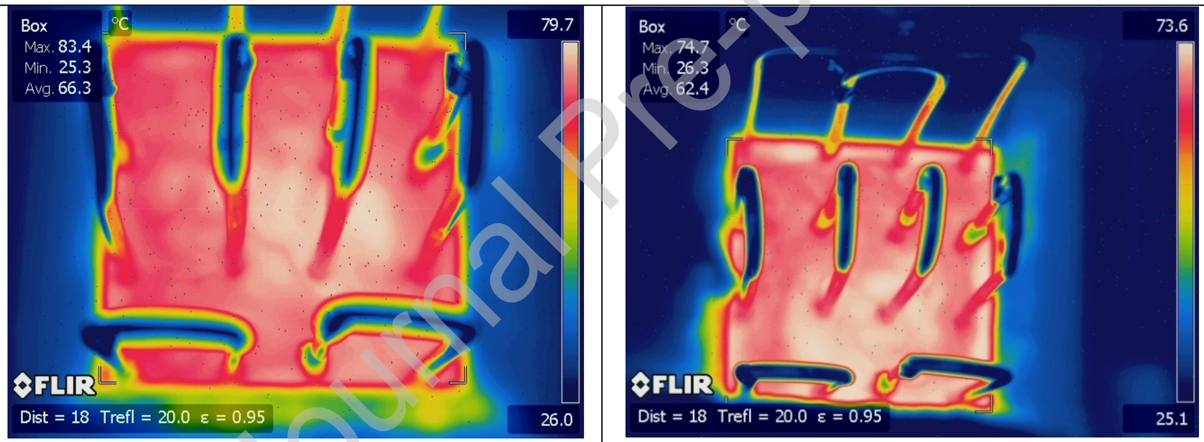

5m/s	8m/s

Figure 25 Thermal images of PCM coupled with 3D-OHP charged with water at different cooling air velocities

A high cooling air velocity benefits the cooling effect; however, increasing the cooling air velocity was accompanied by an increase in energy consumption. An optimal trade-off between cooling air velocity and the temperature of the evaporation section should be established to ensure the electronic components operated in recommended range of temperature with low energy consumption.

Fig. 26 shows the thermal images of PCM/3D-OHP unit at different wind directions. When the system reached a thermal equilibrium stage, the PCM/3D-OHP unit with the side flow arragement exhibited a higher cooling performance. The equilibrium temperature of the electronic component simulator was 100 ℃ when side flow arragement was adopted in cooling the PCM/3D-OHP unit. The equilibrium temperature of the electronic component simulator is 1 ℃ lower than that of the PCM/3D-OHP unit with forward flow arragement. According to the average temperature provided in the thermal images, ΔT_{PCM} was stay unchanged when the wind direction changed from forward flow to side flow. It indicated that the thermal conducitvity of the PCM can not be enhanced by the 3D-OHP at different wind directions. Then the improvement of cooling performance was probably due to the heat transfer performance enhancement in the condensation section. The calculated cooling efficiency was shown in Table 4. The results indicated that the cooling efficiency was slightly improved by using PCM/3D-OHP unit with side flow arragement.

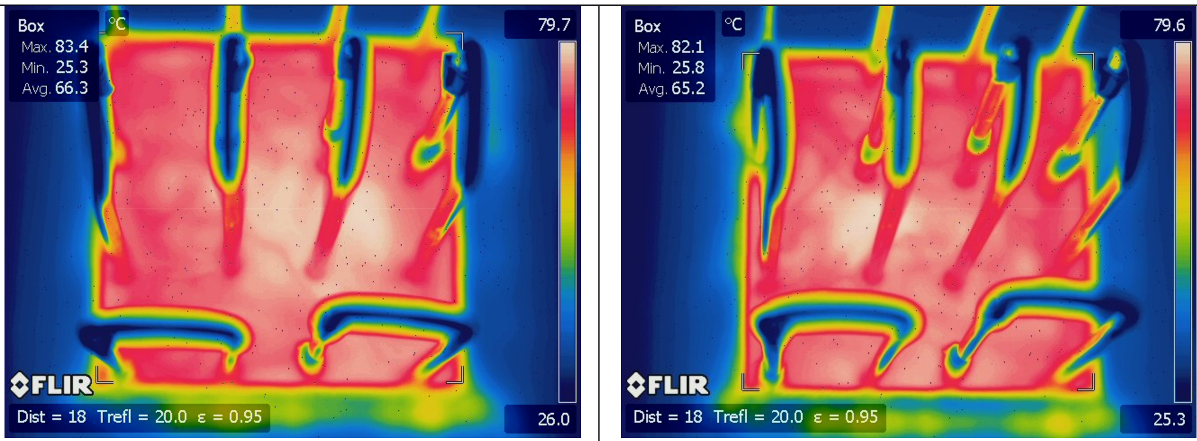

Forward flow	Side flow

Figure 26 Thermal images of PCM coupled with 3D-OHP at different wind directions

Fig. 27 shows the thermal images of PCM/3D-OHP unit with different structures. The copper case was replaced by the rectangle case shown in Fig. 2 b). The size of the copper case was $150 \times 90 \times 60$ mm, the thickness of the copper case was 1 mm. When the system reached a thermal equilibrium stage, the PCM/LSOHP unit has a higher maximum but lower average temperature than the PCM/3D-OHP unit. The equilibrium temperature of the electronic component simulator with PCM/LSOHP unit was 108 ℃, which is 2 ℃ lower than the equilibrium temperature of the electronic component simulator with PCM/3D-OHP unit. According to the average temperatures provided in the thermal images, ΔT_{PCM} decreased from 51.9℃ to 50.4℃. It indicated that the thermal conducitvity of the PCM was enhanced using LSOHP instead of 3D-OHP. Compared with ΔT_{PCM} shown in Table 4, ΔT_{PCM} shown in Table 5 was increased dramatically. It was probably due to the large thermal contact resistance of the rectangle copper case. The calculated cooling efficiency was shown in Table 5, which indicated that the PCM/LSOHP unit exhibited a higher cooling efficiency.

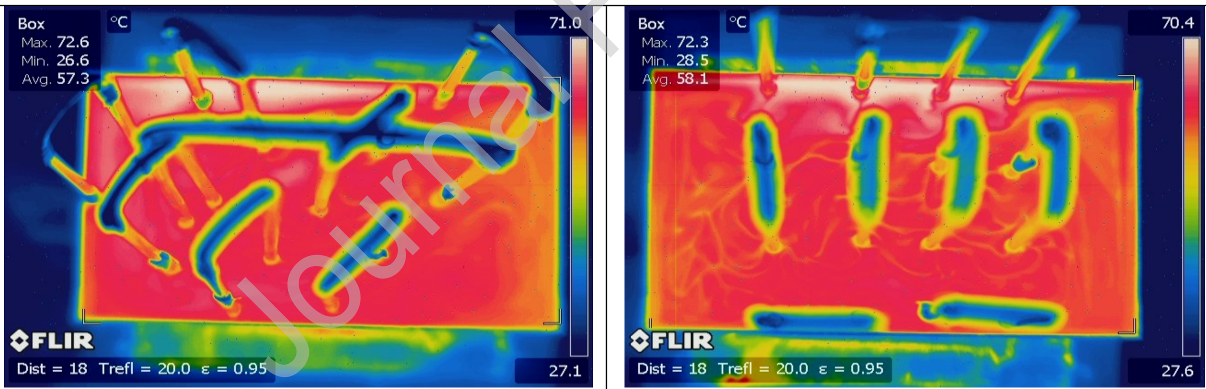

LSOHP	3D-OHP

Figure 27 Thermal images of PCM coupled with 3D-OHP with different structures

Table 4 Cooling efficiency of the PCM/3D-OHP unit under different working conditions

Case	Structure	Velocities (m/s)	Directions	ΔT_{PCM} (℃)	φ(%)
1	3D-OHP	5	Forward flow	34.7	30.1
2	3D-OHP	8	Forward flow	31.6	36.3
3	3D-OHP	5	Side flow	34.8	31

Table 5 Cooling efficiency of the PCM/3D-OHP unit with different structures

Case	Structure	Velocities (m/s)	Directions	ΔT_{PCM} (℃)	φ(%)
1	LSOHP	5	Forward flow	50.7	24.1

2	3D-OHP	5	Forward flow	51.9	22.1

4. Conclusions

Effective electronic cooling is a big challenge with the increasing demand for high-throughput computing of data centres as well as the fast development of battery energy storage. The current air cooling technology is not only energy-intensive but also difficult to cool down the electronic devices. In this paper, an effective cooling technology is proposed for electronic devices by embedding three-dimensional oscillating heat pipe (3D-OHP) into phase change materials (PCMs). The PCMs are used to store the dissipated heat from electronic devices and the 3D-OHP to quickly transport the stored heat to the environment. Experimental study is conducted on the 3D-OHP to optimize its structure with various working parameters such as the cooling air velocity, wind direction and heat input. The cooling performance of PCMs embedded with the 3D-OHP for electronic devices is also investigated in terms of temperature variations and thermal resistance. The main conclusions are shown as follows.

1) The proposed cooling method can control the surface temperature of electronic devices well below 100 ^{o}C, while the conventional air cooling method can only cool the surface temperature to 135 ^{o}C with the same working conditions. Therefore, it is an effective cooling method by using phase change materials (PCMs) embedded with three-dimensional oscillating heat pipe (3D-OHP) for electronic devices. What's more, with the proposed cooling method, thermal resistance by transferring heat to the environment is reduced up to 36.3%.

2) A leaf-shaped structure is designed based on the flow structure found in nature for the three-dimensional oscillating heat pipe. With the same cooling air velocity and wind direction, the leaf-shaped structure contributes to a 2 ^{o}C lower surface temperature on the electronic devices, compared with the typical structure. Thus, the leaf-shaped structure is suggested for the three-dimensional oscillating heat pipe.

3) The operation parameters of the proposed cooling method are optimized. It is found that the three-dimensional oscillating heat pipe achieves the best thermal performance when the filling ratio is in the range of 34-44%. The thermal performance also depends on the cooling air velocity and wind direction. A large cooling air velocity results in a large convective heat transfer coefficient as well as a decrease in the temperature of the evaporation and condensation sections.

Acknowledgments

This study was supported by the National Natural Science Foundation of China (No. 51520105009) and an IGI/ IAS Global Challenges Funding (IGI/IAS ID 3041).

References

[1] Weng Y C, Cho H P, Chang C C, et al. Heat pipe with PCM for electronic cooling[J]. Applied Energy, 2011, 88(5): 1825-1833.

[2] Wu W, Yang X, Zhang G, et al. Experimental investigation on the thermal performance of heat pipe-assisted phase change material based battery thermal management system[J]. Energy Conversion and Management, 2017, 138: 486-492.

[3] Sun W, Huang R, Ling Z, et al. Numerical simulation on the thermal performance of a PCM-containing ventilation system with a continuous change in inlet air temperature[J]. Renewable Energy, 2020, 145: 1608-1619.

[4] Emam M, Ookawara S, Ahmed M. Thermal management of electronic devices and concentrator

photovoltaic systems using phase change material heat sinks: Experimental investigations[J]. Renewable energy, 2019, 141: 322-339

[5] Wang C, Lin T, Li N, et al. Heat transfer enhancement of phase change composite material: Copper foam/paraffin[J]. Renewable Energy, 2016, 96: 960-965.

[6] Nada S A, El-Nagar D H. Possibility of using PCMs in temperature control and performance enhancements of free stand and building integrated PV modules[J]. Renewable Energy, 2018, 127: 630-641.

[7] Ebrahimi A, Hosseini M J, Ranjbar A A, et al. Melting process investigation of phase change materials in a shell and tube heat exchanger enhanced with heat pipe[J]. Renewable Energy, 2019, 138: 378-394.

[8] Behi H, Ghanbarpour M, Behi M. Investigation of PCM-assisted heat pipe for electronic cooling[J]. Applied Thermal Engineering, 2017, 127: 1132-1142.

[9] Krishna J, Kishore P S, Solomon A B. Heat pipe with nano enhanced-PCM for electronic cooling application[J]. Experimental Thermal and Fluid Science, 2017, 81: 84-92.

[10] Zhao J, Rao Z, Liu C, et al. Experimental investigation on thermal performance of phase change material coupled with closed-loop oscillating heat pipe (PCM/CLOHP) used in thermal management[J]. Applied Thermal Engineering, 2016, 93: 90-100.

[11] Qu J, Ke Z, Zuo A, et al. Experimental investigation on thermal performance of phase change material coupled with three-dimensional oscillating heat pipe (PCM/3D-OHP) for thermal management application[J]. International Journal of Heat and Mass Transfer, 2019, 129: 773-782.

[12] Liang J, Gan Y, Li Y, et al. Thermal and electrochemical performance of a serially connected battery module using a heat pipe-based thermal management system under different coolant temperatures[J]. Energy, 2019, 189: 116233.

[13] Jiang Z Y, Qu Z G. Lithium–ion battery thermal management using heat pipe and phase change material during discharge–charge cycle: A comprehensive numerical study[J]. Applied Energy, 2019, 242: 378-392.

[14] Akachi H. Structure of a heat pipe: U.S. Patent 4,921,041[P]. 1990-5-1.Ma H. Oscillating heat pipes[M]. New York: Springer, 2015.

[15] Reay D, McGlen R, Kew P. Heat pipes: theory, design and applications[M]. Butterworth-Heinemann, 2013.Ma H. Oscillating heat pipes[M]. New York: Springer, 2015.

[16] Rittidech S, Donmaung A, Kumsombut K. Experimental study of the performance of a circular tube solar

collector with closed-loop oscillating heat-pipe with check valve (CLOHP/CV)[J]. Renewable Energy, 2009, 34(10): 2234-2238.

[17] Han X, Wang X, Zheng H, et al. Review of the development of pulsating heat pipe for heat dissipation[J]. Renewable and Sustainable Energy Reviews, 2016, 59: 692-709.

[18] Ma H. Oscillating heat pipes[M]. New York: Springer, 2015.

[19] Qu J, Zhao J, Rao Z. Experimental investigation on the thermal performance of three-dimensional oscillating heat pipe. International Journal of Heat and Mass Transfer, 2017, 109: 589-600.

[20] Smoot C D, Ma H B. Experimental investigation of a three-layer oscillating heat pipe[J]. Journal of Heat Transfer, 2014, 136(5): 051501.

[21] Ibrahim O T, Monroe J G, Thompson S M, et al. An investigation of a multi-layered oscillating heat pipe additively manufactured from Ti-6Al-4V powder[J]. International Journal of Heat and Mass Transfer, 2017, 108: 1036-1047.

[22] Thompson S M, Cheng P, Ma H B. An experimental investigation of a three-dimensional flat-plate oscillating heat pipe with staggered microchannels[J]. International Journal of Heat and Mass Transfer, 2011, 54(17-18): 3951-3959.

[23] Bejan A, Zane J P. Design in nature[J]. Mechanical Engineering Magazine Select Articles, 2012, 134(06): 42-47.

[24] Rubio-Jimenez C A, Hernandez-Guerrero A, Cervantes J G, et al. CFD study of constructal microchannel networks for liquid-cooling of electronic devices[J]. Applied Thermal Engineering, 2016, 95: 374-381.

[25] Zhang C, Lian Y, Hsu C H, et al. Investigations of thermal and flow behavior of bifurcations and bends in fractal-like microchannel networks: Secondary flow and recirculation flow[J]. International Journal of Heat and Mass Transfer, 2015, 85: 723-731.

[26] Xu P, Wang X Q, Mujumdar A S, et al. Thermal characteristics of tree-shaped microchannel nets with/without loops[J]. International Journal of Thermal Sciences, 2009, 48(11): 2139-2147.

[27] Luo L, Tian F, Cai J, et al. The convective heat transfer of branched structure[J]. International Journal of Heat and Mass Transfer, 2018, 116: 813-816.

[28] Nayak B B, Chatterjee D. Convective heat transfer in slurry flow in a horizontal Y-shaped branch pipe[J]. Powder technology, 2017, 318: 46-61.

[29] Zheng J, Wang J, Chen T, et al. Solidification performance of heat exchanger with tree-shaped fins[J]. Renewable Energy, 2019.

[30] Taft B S, Williams A D, Drolen B L. Review of pulsating heat pipe working fluid selection. Journal of Thermophysics and Heat Transfer, 2012, 26(4): 651-656.

[31] Charoensawan P, Terdtoon P. Thermal performance correlation of horizontal closed-loop oscillating heat pipes[C]//2007 9th Electronics Packaging Technology Conference. IEEE, 2007: 906-909.

List of figure captions

Fig. 1 Schematic of the three-dimensional oscillating heat pipe (3D-OHP) and the points measured during the test

Fig. 2 Schematic of the leaf-shaped three-dimensional oscillating heat pipe (LSOHP)

Fig. 3 Design and constructal law of the leaf-shaped three-dimensional oscillating heat pipe (LSOHP)

Fig. 4 Schematic of the test room

Fig. 5 Experimental apparatus of the test unit for three-dimensional oscillating heat pipes (3D-OHP)

Fig. 6 Wind direction of the three-dimensional oscillating heat pipes (3D-OHP)

Fig. 7 Wind direction of the leaf-shaped three-dimensional oscillating heat pipe (LSOHP)

Fig. 8 Schematic of the PCM/3D-OHP unit

Fig. 9 Schematic of the test room with under floor air distribution

Fig. 10 Schematic of the test room with under floor air distribution

Fig. 11 Temperature oscillations of the 3D-OHPs at different FRs

Fig. 12 Temperature variations of the 3D-OHPs at different FRs in the evaporation section

Fig. 13 Thermal resistance of the 3D-OHPs at different FRs

Fig. 14 Temperature variations of the 3D-OHPs at different cooling air velocities

Fig. 15 Thermal resistance of the 3D-OHPs at cooling air velocities

Fig. 16 Air flow through the 3D-OHP in staggered arrangement

Fig. 17 Temperature variations of the 3D-OHPs at different wind directions

Fig. 18 Thermal resistance of the 3D-OHPs at different wind directions

Fig. 19 Temperature oscillations of the LSOHP at different wind directions

Fig. 20 Temperature variations of the LSOHP at different wind directions

Fig. 21 Thermal resistance of the LSOHP at different wind directions

Fig. 22 Temperature variations of the LSOHP at different air velocities

Fig. 23 Thermal resistance of the LSOHP at different air velocities

Fig. 24 Thermal resistance model of the PCM/3D-OHP unit

Fig. 25 Thermal images of PCM coupled with 3D-OHP charged with water at different cooling air velocities

Fig. 26 Thermal images of PCM coupled with 3D-OHP at different wind directions

Fig. 27 Thermal images of PCM coupled with 3D-OHP with different structures

List of table captions

AUTHOR DECLARATION

We wish to confirm that there are no known conflicts of interest associated with this publication and there has been no significant financial support for this work that could have influenced its outcome. We confirm that the manuscript has been read and approved by all named authors and that there are no other persons who satisfied the criteria for authorship but are not listed. We further confirm that the order of authors listed in the manuscript has been approved by all of us. We confirm that we have given due consideration to the protection of intellectual property associated with this work and that there are no impediments to publication, including the timing of publication, with respect to intellectual property. In so doing we confirm that we have followed the regulations of our institutions concerning intellectual property.

We understand that the Corresponding Author is the sole contact for the Editorial process (including Editorial Manager and direct communications with the office). He is responsible for communicating with the other authors about progress, submissions of revisions and final approval of proofs. We confirm that we have provided a current, correct email address which is accessible by the Corresponding Author and which has been configured to accept email from yunzhiseu@outlook.com.

Signed by all authors as follows:

Xiaorong Zhang

Yunzhi Ling

Author contributions:
Yunzhi Ling designed the experimental device in laboratory, and photographed and analyzed the heat pipes shown in relevant figures. This paper was guided by Xiao-song Zhang. Yun-zhi Ling worked with Feng Wang and Xiao-hui She on the writing and revision.

Study of the performance of PCM coupled with three-dimensional oscillating heat pipes with different structures

Highlights

1. The effect of various factors on 3D-OHP performance was investigated
2. The best performance was observed for an FR in the range of 34–44%
3. A LSOHP exhibits the better cooling performance
4. An optimized cooling performance was obtained using PCM/LSOHP unit